

Surface local-field effect on the optical properties of GaAs(110) and GaP(110)

C. M. J. Wijers

Twente University of Technology, P.O. Box 217, 7500 AE Enschede, The Netherlands

R. Del Sole

Physics Department, Second University of Rome "Tor Vergata," v.E. Carnevale, I-00173 Roma, Italy

F. Manghi

Physics Department, University of Modena, v.A. Campi 217/A, I-41100 Modena, Italy

(Received 16 July 1990; revised manuscript received 26 November 1990)

A method for the calculation of the surface local-field effect on reflectance has been developed. It also takes into account the different polarizabilities of surface and bulk. Application has been made to GaAs(110) and GaP(110), starting from first-principles one-electron calculations of surface optical properties. The inclusion of local fields has important—yet not drastic—effects on line shapes of reflectance-anisotropy and differential-reflectivity measurements.

I. INTRODUCTION

The measurement of the reflectance anisotropy (RA) of cubic crystals is an important tool for the investigation of surface structure.¹⁻³ Since the bulk optical properties of cubic crystals are isotropic, any observed anisotropy must be related to the lower symmetry of the surface. Some of these surface-induced optical anisotropies are due to adsorbed films, surface states, or surface reconstruction. However, an intrinsic reflectance anisotropy has been measured for the natural (110) surfaces of Si and Ge,² where no optically active surface state is expected in the frequency range of interest. This anisotropy has been interpreted as arising from the surface-local-field (SLF) effect:⁴ the surface is assumed to have the same isotropic polarizability as the bulk, but to respond to different local fields for different light polarizations. This yields a calculated RA in agreement with experiment.² A concurring reason for RA may be, however, the anisotropy of the surface polarizability itself, arising from the reduced symmetry of Si and Ge, as well as of III-V compounds, (110) surfaces. It has been shown by a tight-binding random-phase-approximation (RPA) calculation⁵ that for Si(110):H, the latter effect gives a RA of the same order of magnitude as that due to the SLF effect. The hydrogen coverage was meant to mimic the native oxide layer present at natural surfaces, on which the experiments were carried out. However, the resulting line shape is different from the experimental one.

RPA calculations have also been carried out for GaAs and GaP(110) surfaces.⁶⁻⁹ The computed RA and the differential reflectance (DR) (the difference between the reflectivity of the clean surface and that after chemisorption) have been compared with experiment.^{3,10,11} The agreement—yet reasonable in some cases—is not complete. It may be argued that some of the discrepancies arise from many-body effects. Among these, the most important are the excitonic effect, arising from the

electron-hole interaction, and the SLF effect, arising from the microscopic structure of the crystal. In this paper we want to explore the SLF effect on the optical properties. To this aim, we neglect excitonic effects (more precisely, we neglect the difference between surface and bulk electron-hole interaction), and study local-field effects within the dipole picture of crystal polarizability.^{4,12} The polarizabilities of bulk and surface dipoles are extracted from bulk and slab RPA calculations.^{8,9} We compute the electromagnetic field generated by the dipoles in a slab in response to the external (incident wave) field. In this way, the reflection and transmission coefficients are computed. Then the reflectance of a semi-infinite crystal is found from slab optical properties. Such an approach has the advantage of avoiding the cumbersome solution of light-propagation equations near the surface (usually carried out perturbatively^{13,14}) involved in the usual approach, but relies from the beginning on the dipole picture. (A derivation of this picture from linear-response theory has been recently given.¹⁵) It yields the same results as the usual approach when surface resonances are weak enough that the perturbative approach is reliable, but it can embody higher-order effects without further effort.

The method of calculation is described in Sec. II. The results, discussed in Sec. III, show that local-field effects do not qualitatively modify the RPA optical line shapes. Other reasons should be invoked to explain the discrepancies with respect to experiments. The conclusions of this work are summarized in Sec. IV.

II. METHOD OF CALCULATION

A. Dipole theory for thin slabs

A beam of electromagnetic radiation impinges on a slab of N (110) atomic layers of a III-V semiconductor (in particular, GaP and GaAs will be considered in this paper). The z direction corresponds to the [110] direction,

perpendicular to the planes of the slab. We divide the specimen under consideration into a number of polarizable units (cells) with index i , dipole strength \mathbf{p}_i , and polarizability α_i . The dipole induced at the i cell is

$$\mathbf{p}_i = \vec{\alpha}_i \cdot \mathbf{E}_{\text{loc},i}, \quad (1)$$

where $\mathbf{E}_{\text{loc},i}$ is the local field and $\vec{\alpha}_i$ is the polarizability tensor. Strictly speaking, the off-diagonal terms $\vec{\alpha}_{ij}$ relating the dipole induced at \mathbf{r}_i to the local field at \mathbf{r}_j should also be included.¹⁵ However, following the approach of Mochan and Barrera⁴ and for sake of simplicity, we consider here only diagonal ($i=j$) polarizabilities. The dipoles \mathbf{p}_i give rise to Hertz potentials,¹⁶ from which the induced electric field can be obtained as

$$\mathbf{E}_i(\mathbf{r}, t) = \nabla(\nabla \cdot \mathbf{Z}_i) - \left[\frac{\partial^2 \mathbf{Z}_i}{\partial t^2} \right] / c^2, \quad (2)$$

with

$$\mathbf{Z}_i(\mathbf{r}, t) = (\mathbf{p}_i / |\mathbf{r} - \mathbf{r}_i|) \exp[i(k|\mathbf{r} - \mathbf{r}_i| - \omega t)], \quad (3)$$

where $k = \omega/c$. The external and induced fields give rise to the total field

$$\mathbf{E}_{\text{tot}}(\mathbf{r}, t) = \mathbf{E}_{\text{ext}}(\mathbf{r}, t) + \sum_i \mathbf{E}_i(\mathbf{r}, t). \quad (4)$$

Because of parallel translational symmetry, we have the relation

$$\mathbf{p}_{\mathbf{R},n} = \exp(i\mathbf{k} \cdot \mathbf{R}) \mathbf{p}_{\mathbf{0},n} \quad (5)$$

between dipoles in the layer n , where $\mathbf{R} = (R_x, R_y, 0)$ spans the two-dimensional (2D) lattice and \mathbf{k} is the wave vector of the incident light. (In the case of normal incidence, for which calculations will be carried out in this paper, \mathbf{R} and \mathbf{k} are orthogonal, so that all dipoles in the same layer have the same strength.) The infinitely many unknown dipole strengths $\mathbf{p}_{\mathbf{R},n}$ reduce to a single one $\mathbf{p}_{\mathbf{0},n}$ for each plane, located at the origin \mathbf{r}_n of the lattice belonging to the n plane. (The index $\mathbf{0}$ will be omitted in the following.) Straightforward combination of these relations yields the following system of equations:

$$\mathbf{p}_n = \vec{\alpha}_n \cdot \left[\mathbf{E}_{\text{ext},n} + \sum_j \vec{\mathbf{F}}_{nj} \cdot \mathbf{p}_j \right], \quad (6)$$

$$\vec{\mathbf{F}}_{nj} = (\nabla^T \nabla + k^2 \vec{\mathbb{1}}) S_j(\mathbf{r}, k) \Big|_{\mathbf{r}=\mathbf{r}_n}, \quad (7)$$

$$S_j(\mathbf{r}, k) = \sum_{\mathbf{R}}^{(\prime)} \exp(i\mathbf{k} \cdot \mathbf{R}) \exp(ik|\mathbf{r} - \mathbf{R} - \mathbf{r}_j|) / |\mathbf{r} - \mathbf{R}_j|, \quad (8)$$

where the term in the large parentheses in (6) is the local field at the origin of the n plane. The incident field driving the entire process enters Eq. (6) as $\mathbf{E}_{\text{ext},n}$. Vector combinations of the $\mathbf{v}^T \mathbf{v}$ indicate the corresponding direct product subtensor, the dyad. Equation (8) defines the lattice sums $S_j(\mathbf{r}, k)$. The prime means that in the case $\mathbf{r} = \mathbf{r}_j$, the term with vanishing denominator must be omitted.

The main problem of the dipole theory is to calculate

$\vec{\mathbf{F}}_{nj}$. The intraplanar ($n=j$) terms, already given in Ref. 12, have been calculated by a straightforward extension of the method of Vlieger,¹⁷ originally devised for square lattices, to rectangular lattices. We find

$$a^3 \vec{\mathbf{F}}_{nn} = \vec{c}_{\text{stat}} + 2\pi i a (k^2 \vec{\mathbb{1}} - \mathbf{k}_{\parallel}^T \mathbf{k}_{\parallel} - \mathbf{k}_z^T \mathbf{k}_z) / (\beta |k_z|), \quad (9)$$

where $a = a^c / \sqrt{2}$ (a^c is the lattice constant) and $\beta = \sqrt{2}$. In deriving (9), the sum outside a circle of radius r_0 (much larger than a and much smaller than k^{-1}) has been transformed into an integral.¹⁷ The calculated integral and the sum inside the circle are expanded up to the first order in kr_0 and then the zeroth-order integral term is converted back into a sum. The final result contains the static all-plane dipole sum

$$\vec{c}_{\text{stat}} = a^3 \sum_{\mathbf{R}}^{(\prime)} (\mathbf{R}^T \mathbf{R} - R^2 \vec{\mathbb{1}}) / R^5 \quad (10)$$

plus the term linear in k appearing in (9). Terms of the order $(kr_0)^2$ are neglected in this way, altogether with the Lorentz damping, proportional to k^3 .¹⁷ Neglecting the latter term is well justified in solids, where more important damping mechanisms are present, such as, for instance, interaction with phonons.

The value of \vec{c}_{stat} can be easily computed by brute force (i.e., direct summation) or by a modified Hoff-Benson method.^{18,19} The result is

$$\vec{c}_{\text{stat}} = \begin{bmatrix} 4.7901 & 0 & 0 \\ 0 & 0.9060 & 0 \\ 0 & 0 & -5.6961 \end{bmatrix}. \quad (11)$$

Next we have to evaluate the off diagonal terms. In this case it is more convenient to convert the sum over the direct lattice into a sum over the reciprocal lattice. We find

$$S_j(\mathbf{r}, k) = (2\pi / A_0) \sum_{\mathbf{G}} \exp[i(\mathbf{k}_{\parallel} + \mathbf{G}) \cdot \mathbf{r}] \times \exp(-\kappa_{\mathbf{G}} |z|) / \kappa_{\mathbf{G}}, \quad (12)$$

$$\kappa_{\mathbf{G}} = (|\mathbf{k}_{\parallel} + \mathbf{G}|^2 - k^2)^{1/2}, \quad (13)$$

where \mathbf{G} is a vector of the reciprocal 2D lattice and A_0 is the cell area. It should be noticed that (12) cannot be used for $z=0$. [For this reason we had to carry out the cumbersome calculation in real space in order to get the intraplanar term (9).] For neighboring planes it is also slowly convergent, but it is still much quicker than direct calculation according to (8). After that, it readily approaches the speed of an analytical expression. The non-analytic behavior at small k in the term linear in k of the dipole-dipole interaction F_{nj} , clearly apparent in the intraplanar term (9), is present also in the interplanar terms: in this case, it is contained in the term with $\mathbf{G}=\mathbf{0}$ of the sum (12), which depends differently on \mathbf{k}_{\parallel} and k_z .

Once the results of (9) and (12) are obtained, we are left with a system of $3N$ linear equations in the $3N$ unknowns, the components of the \mathbf{p}_n 's. Surface effects are embodied in the dipole-dipole interplanar interaction, which is perturbed by the missing layers (this is the surface-local-field effect of Mochan and Barrera⁴), and in the layer-

dependent dipole polarizabilities $\vec{\alpha}_n$. The solution of the system is

$$\mathbf{p}_n = \sum_j (\vec{A}^{-1})_{nj} \cdot \mathbf{E}_{\text{ext},j}, \quad (14)$$

where

$$\vec{A}_{nj} = \delta_{nj} \vec{\alpha}_n^{-1} - \vec{F}_{nj}. \quad (15)$$

The dipole strengths \mathbf{p}_n together build a complete description of the optical response of the slab under irradiation by a light wave. The measurable quantities are functions of the \mathbf{p}_n 's.

We solve the linear system (6) by numerical inversion of the $3N \times 3N$ matrix \vec{A}_{nj} . This is possible, of course, to the extent that N is not too large. An alternative method, suitable for thicker slabs, is the expansion of the total field in normal modes inside the slab.²⁰ Since both methods are meant to solve the linear system (6), they are equivalent to the extent that they use the same truncation of the interplanar dipole-dipole interaction.

B. Dipole polarizabilities

The next step is to determine the polarizabilities of surface and bulk dipoles. We start from a pseudopotential calculation of electronic states and of the RPA dielectric constant of bulk GaAs and GaP, as described in Ref. 9. Then we use the same approach for repeated slabs of $N = 15$ GaAs or GaP(110) layers separated by nine missing layers.⁹ In order to minimize the gap underestimates involved in the local-density-functional (LDA) approximation,^{21,22} we have used the Slater, rather than the Kohn-Sham²³, exchange potential. Calculated bulk gaps (1.5 eV for GaAs, 3.1 eV for GaP) are in good agreement with real ones (1.5 eV for GaAs, 2.8 eV for GaP).⁹ It is not clear, however, whether gaps between surface states are well reproduced or not, since conflicting experimental findings on the energy of empty surface states have been presented.^{24,25} The output of the calculation is the integral $I(\omega)$ of the slab dielectric susceptibility $\epsilon(\omega; z, z')$ over z and z' . Neglecting nonlocality and assuming that the first N_s layers near each surface have dielectric constant ϵ_s , while the inner layers have the bulk dielectric constant, we get

$$\epsilon_s(\omega) = I(\omega)/(2N_s d_l) - [N/(2N_s) - 1] \epsilon_b(\omega), \quad (16)$$

where d_l is the interlayer spacing. Because of the symmetry of the (110) surface, ϵ_s will be different for light polarized along [001] or [1 $\bar{1}$ 0]. The choice of N_s is dictated by the physical requirement of a thin surface layer, which is, however, contrasted by the appearance of a negative imaginary part of ϵ_s for too small N_s . We choose $N_s = 3$, which is the smallest value for which the imaginary part of ϵ_s is positive in the frequency range 0–13 eV.

We extract the bulk dipole polarizability from the calculated RPA dielectric constant. The Lorentz-Lorenz formula relates the former to the actual (macroscopic) dielectric constant,^{26,27} which is different from the RPA one. It is, however, known that such a difference, due to many-body effects, is quite small in semiconductors:²⁸

peak energies are weakly affected, while larger changes occur in line shapes. Therefore, a zeroth-order approximation, used here, is to identify the RPA polarizability with the macroscopic one and to derive from it the dipole polarizability via the Lorentz-Lorenz equation. This procedure yields a relation between the RPA and dipole polarizabilities. Because of the very definition of the dipole (called “atomic” in Refs. 15 and 27) polarizability, such a relation does not involve the dipole-dipole interaction, but only the short-range interactions. For instance, within a simplified two-band model,²⁷ we have

$$\alpha^{\text{dip}}/\Omega = \alpha^{\text{RPA}} [1 - (V_0 - V_x/2)\Omega\alpha^{\text{RPA}}/f^2]. \quad (17)$$

Here V_0 and V_x are the Coulomb and exchange interaction in the same cell, Ω is the cell volume, and f is the matrix element of the dipole operator between the Wannier functions of the two bands. Equation (17) is coincident with the inverse Lorentz-Lorenz relation when $V_0 - V_x/2 = 4\pi f^2/3\Omega$. This implies the vanishing of $(V_0 - V_x/2 - 4\pi f^2/3\Omega)$, which is the combined effect of intracell electron-hole interactions and of the long-range dipole-dipole interactions. It is in this very case that the macroscopic and RPA dielectric constants coincide, as was assumed from the beginning. We assume that the same relation holds near the surface and again derive the polarizability of the dipoles in the surface layers from ϵ_s , computed within the RPA, through the Lorentz-Lorenz equation. By using the same relation in bulk and near the surface, we simply assume that the electron-hole interaction is not modified by the surface itself.

In order to compare the present approach with that of Mochan and Barrera,⁴ based on the solution of light-propagation equations, we repeat the calculation for Si(110):H, already performed in Ref. 15 according to the latter approach. We take from Ref. 15 surface and bulk dipole polarizabilities, which account to some extent for excitonic effects.

C. Remote fields: Reflectance and transmittance

The remote fields can be obtained by applying (7) and (12) along the line of calculation shown in Ref. 17. We find for the reflected and transmitted beam

$$\mathbf{E}^R(\mathbf{r}, t) = (2\pi i/\beta |k_z| a^2) \times (k^2 \vec{1} - \mathbf{k}_r^T \mathbf{k}_r) \cdot \mathbf{P}^R \exp[i(\mathbf{k}_r \cdot \mathbf{r} - \omega t)], \quad (18)$$

$$\mathbf{E}^T(\mathbf{r}, t) = [\mathbf{E}_0 + (2\pi i/\beta |k_z| a^2) \times (k^2 \vec{1} - \mathbf{k}^T \mathbf{k}) \cdot \mathbf{P}^T] \exp[i(\mathbf{k} \cdot \mathbf{r} - \omega t)], \quad (19)$$

where $\mathbf{E}_0 \exp[i(\mathbf{k} \cdot \mathbf{r} - \omega t)]$ is the external (normally incident) field, \mathbf{k}_r is the wave vector of the reflected wave, and

$$\mathbf{P}^R = \sum_j \exp(-i\mathbf{k}_r \cdot \mathbf{r}_j) \mathbf{p}_j, \quad (20)$$

$$\mathbf{P}^T = \sum_j \exp(-i\mathbf{k} \cdot \mathbf{r}_j) \mathbf{p}_j. \quad (21)$$

Finally, we find the complex reflectivity and transmittivi-

ty at normal incidence:

$$r = (2\pi i / \beta |k_z| a^2) k^2 (\mathbf{E}_0 \cdot \mathbf{P}^R / |\mathbf{E}_0|), \quad (22)$$

$$t = 1 + (2\pi i / \beta |k_z| a^2) k^2 (\mathbf{E}_0 \cdot \mathbf{P}^T / |\mathbf{E}_0|). \quad (23)$$

D. Reflectance of a semi-infinite crystal

The discrete dipole model treated until now is not suited for the description of semi-infinite systems, hence the results obtained so far cannot be compared with experiments. However, the slab, in principle, can be made so thick that most of its interior is bulklike. In that case, a classical continuous description can be used to extract the required results for a semi-infinite crystal from slab calculations.

Inside the slab, where surface effects are not important, light propagates according to the wave-vector q_z given by

$$q_z = (\omega/c) \epsilon_b^{1/2}(\omega). \quad (24)$$

We can find the reflectivity and transmissivity of a slab of thickness d by summing the contributions of multiple reflections of waves propagating with wave-vector $\pm q_z$. This approach is similar to that of Ref. 29, with the difference that we are here considering field amplitudes (and not their square moduli) in order to fully account also for interference effects, which cannot be neglected in thin slabs. After some algebra we arrive at the relation

$$r(d) = r + r' \exp(iq_z d) t(d). \quad (25)$$

Here r means the reflectivity of a semi-infinite sample from vacuum to bulk—the required quantity—while r' is the reflectivity from bulk to vacuum. Surface effects are fully included in r and r' , according to the approach of Refs. 14 and 29. If one uses (25) for two different layers of thickness d_A and d_B , respectively, the reflectance of a semi-infinite crystal turns out to be

$$r = \{t(d_A) r(d_B) - \exp[iq_z(d_B - d_A)] t(d_B) r(d_A)\} / \{t(d_A) - \exp[iq_z(d_B - d_A)] t(d_B)\}. \quad (26)$$

In the following we use $d_B = 54$ layers and $d_A = 38$ layers. The convergence has been checked by using $d_B = 38$ layers and $d_A = 20$ layers, finding practically no difference.

The method used in this subsection makes the contact with the normal-mode expansion, used, for instance, by Grindlay.²⁰ We are actually considering a single, long-wavelength, normal mode deep inside the slab, whose amplitude is determined, rather than by the boundary equations of Ref. 20, which are in turn determined by the microscopic structure of the surfaces, directly by the numerical solution of the linear system (6) near the surfaces. It can be shown that, within a broad absorption band such as that considered here, additional long-wavelength modes are not present, while short-wavelength normal modes have little effect on the optical properties.²⁰

E. Test of the method

We have tested our method of computing the SLF effect on reflectance in the case of Si(110):H. The calculated RA has been compared with that computed, according to the approach of Mochan and Barrera, in Ref. 15. The two approaches yield practically identical results. This confirms the validity of our method and also makes us sure that the condition of relatively weak surface resonances, needed for the validity of the Mochan-Barrera approach, is fulfilled.

III. RESULTS

Let us discuss now the RA of the clean GaAs(110) surface. Figures 1(a) and 1(b) show the surface contributions to reflectance of x - and y -polarized normally incident light, respectively. (We take the x axis parallel to $[1\bar{1}0]$ and the y axis parallel to $[001]$.) The overall effect of

SLF's is to reduce the reflectance (mostly of y light, i.e., of light polarized normally to the $[1\bar{1}0]$ chains). This can be understood as follows: the dipole-dipole interaction shifts the main resonance of the polarizability to low energies. This is clear from the Lorentz-Lorenz formula, and can be directly verified by comparing the bulk macroscopic polarizability, embodying the dipole-dipole interaction, with the atomic one: the latter has a much larger resonance energy, and, by consequence, a much lower static value (about 2 versus about 10). At surfaces, the missing half crystal reduces the dipole-dipole interaction and the associated shift, so that the surface macroscopic polarizability is overall shifted, with respect to the RPA one, to higher energies. This implies a reduction of low-energy features, such as those shown in Fig. 1. This effect is larger for the light polarized along y , because the yy component of the in-plane static pole sum \vec{c}_{stat} [see (11)] is much smaller than the bulk (cubic) value of $4\pi/3$. This means that the effect of missing layers on the local field at the surface is larger for y polarization than for x polarization: actually, in the latter case, the in-plane sum c_{stat} is very close to the bulk value, implying a less important effect of missing layers.

The RA is shown in Fig. 1(c). As a consequence of the different reductions for the two polarizations, the peak at 3.6 eV is enhanced, with respect to RPA, by the SLF effect. The agreement of GaAs(110) RA with the experiment carried out by Berkovits *et al.*¹⁰ is reasonable. The inclusion of local-field effects, however, does not improve the agreement.

The surface contribution to the reflectance of GaP(110) is shown in Fig. 2. Also, in this case, the overall reduction of low-energy reflectance structures by local-field effects is apparent in Figs. 2(a) and 2(b). The RA in Fig.

2(c) shows an enhancement in the energy range around 4 eV. The agreement with experiment is worse in this case, and the SLF effect is not big enough to improve it.

In both cases, the SLF contribution to RA is not dramatic. This might seem to contrast the case where no anisotropy is present within RPA (Refs. 4 and 30), where the SLF effect yields a RA of the order of 1%. The paradox, however, is only apparent, since SLF-induced changes of RA are still of this order, even though they are definitely smaller than the RPA contribution. The main SLF effect on the RA of III-V compounds, namely the enhancement in the valley between the two main peaks, centered at 3.1 (4) eV in GaAs (GaP), is similar but smaller to that found for Si(110):H.¹⁵ A similar effect, namely an enhancement of $R_x - R_y$ with respect to the RPA value (zero, in this case), is also found when surface dipoles are assumed to have the same polarizability as bulk ones.^{4,30}

Let us now discuss differential reflectivity. In experiments, oxygen chemisorption is often used to saturate surface states.³ In our calculation, instead, we mimic the

chemisorbed surface by a H monolayer.^{6,7,9} This can cause some of the discrepancies found between theory and experiment. The calculated DR of GaP(110) is shown in Fig. 3 for x polarization [Fig. 3(a)], y polarization [Fig. 3(b)], and for the RA [Fig. 3(c)]. Again, the SLF effect reduces the reflectance (low-frequency) structures; in this case the agreement with experiment, already good in RPA, is improved by SLF effects.

The DR of GaAs(110) is shown in Fig. 4. The SLF effect is similar to that in GaP; an overall reduction of low-frequency structures. However, agreement with experiment is only qualitative, and local-field effects do not improve it.

IV. CONCLUSIONS

In this paper we have described a method to compute the SLF effect on optical properties. It is based on the dipole picture of crystal optics: it consists of calculating the response of the dipoles in a slab to the incident radiation. From slab reflectance and transmission, the reflectance of a semi-infinite crystal is obtained. The cumbersome solution of light-propagation equations near the surface involved in the usual approach^{4,13,14} is there-

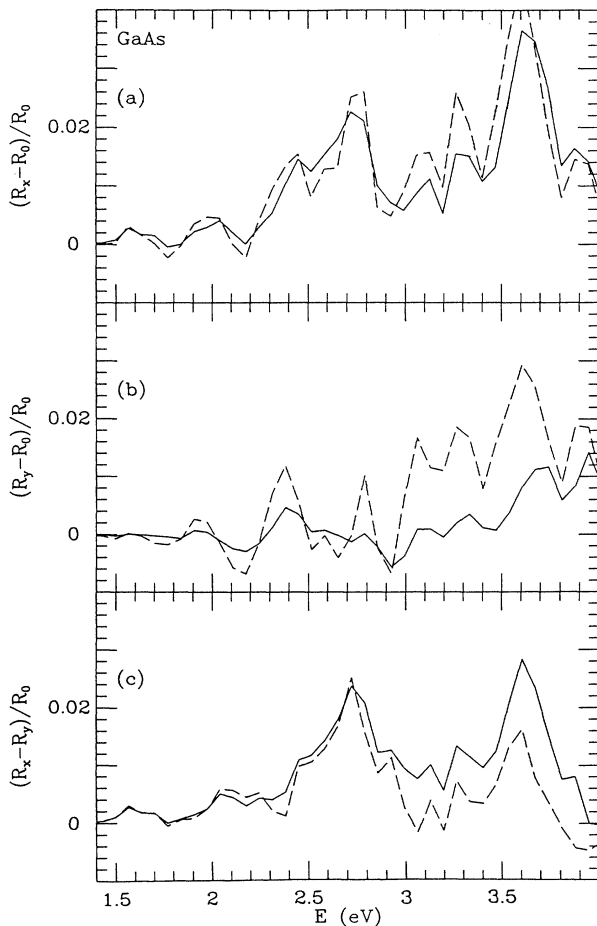


FIG. 1. Surface contribution to reflectance computed for GaAs (110). (a) Light polarized along $[1\bar{1}0]$ (x); (b) light polarized along $[001]$ (y); (c) the difference. Dashed lines, one-electron RPA; Solid lines, the surface-local-field effect.

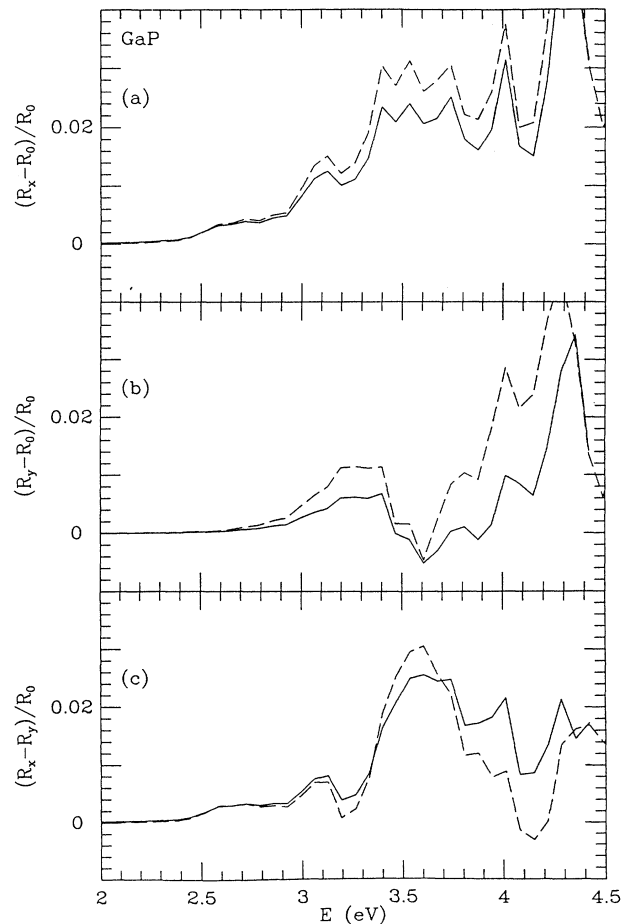


FIG. 2. The same as Fig. 1 for GaP(110).

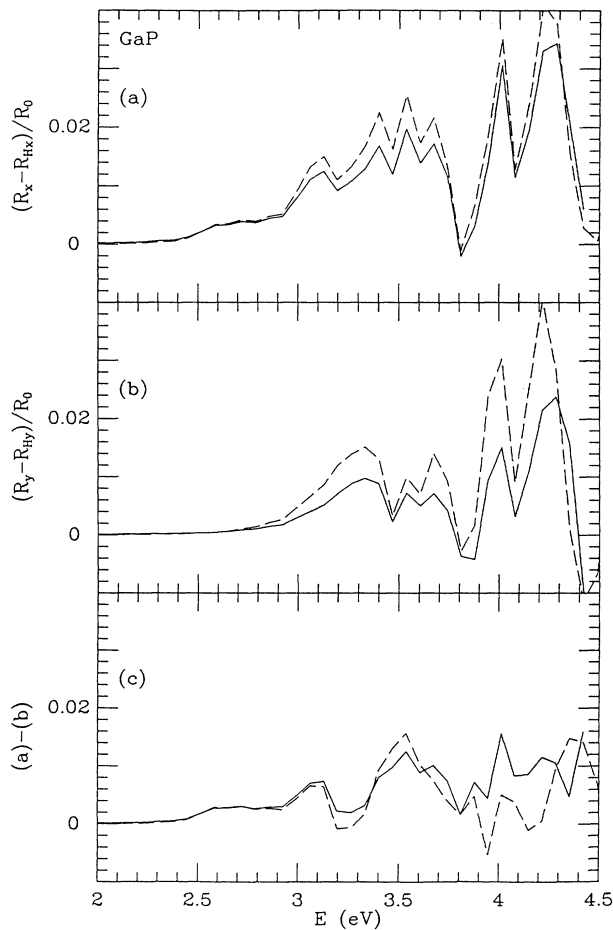


FIG. 3. Calculated differential reflectance of GaP(110). (a) Light polarized along $[1\bar{1}0]$ (x); (b) light polarized along $[001]$ (y); (c) the difference. Dashed lines, the one-electron RPA; Solid lines, inclusion of the surface local-field effect.

fore avoided. The soundness of the method has been checked by comparison with calculations carried out according to the other approach.

We have applied our method to GaAs and GaP(110). The agreement between RPA calculations and experiment is quite good for peak energies, but is not always so for line shapes. The inclusion of the SLF effect yields an overall reduction of low-frequency structures, especially for light polarized along y , perpendicular to the $[1\bar{1}0]$ chains. In RA, however, since the difference $R_x - R_y$ is of interest, these structures are amplified by the SLF effect. This effect may substantially modify the line shapes, even though it has little influence on the energies of the main structures. We have found that, in the case of GaP(110) DR, the inclusion of local-field effects improves the comparison with experiment. In the other cases, no relevant improvement is obtained.

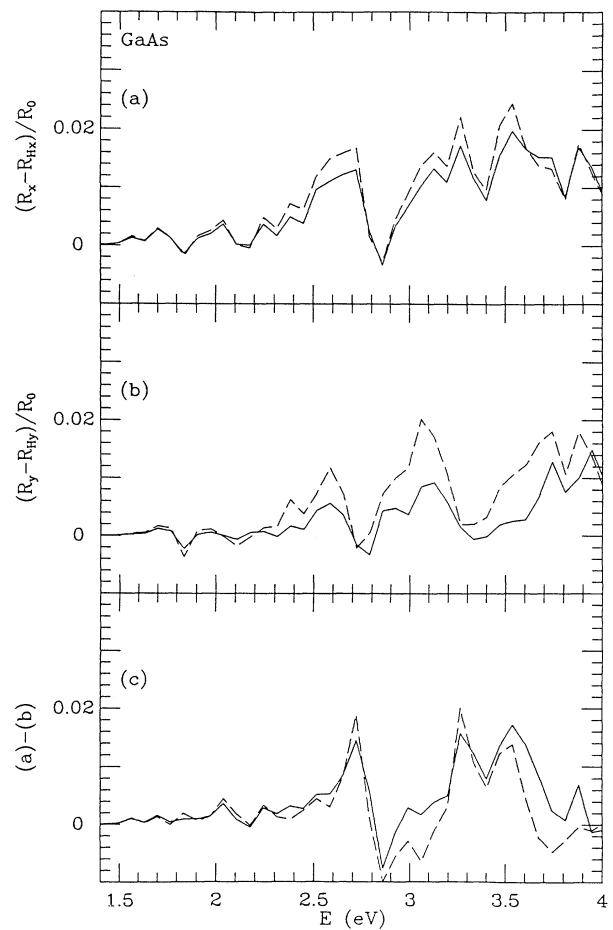


FIG. 4. The same as Fig. 3 for GaAs(110).

The poor agreement between theory and experiment found in some cases may be due to several factors, such as to the mimicking of the oxidized surfaces involved in DR experiments by H-covered surfaces, and the uncertainties in the determination of the one-electron states involved in the RPA calculations. The last uncertainties have to do with the gap problem associated with the local-density-functional approach: as is well known, the LDA underestimates band gaps in semiconductors by about 50%, and the use of Slater (instead of Kohn-Sham) exchange is a simple—yet empirical—way to get correct bulk gaps. Unfortunately, it is not clear whether this occurs for gaps between surface (or between surface and bulk) states, where residual discrepancies of the order of 0.6 eV might be present.^{9,31} Other possible reasons might be associated with surface exciton effects, as well as with the nonlocality of the self-energy operator, which has been found to substantially affect the static dielectric constant of Si and Ge.^{32,33}

- ¹S. Selci, P. Chiaradia, F. Ciccacci, A. Cricenti, N. Sparvieri, and G. Chiarotti, *Phys. Rev. B* **31**, 4096 (1985).
- ²D. E. Aspnes and A. A. Studna, *Phys. Rev. Lett.* **54**, 1956 (1985).
- ³S. Selci, F. Ciccacci, A. Cricenti, A. C. Felici, C. Goletti, and P. Chiaradia, *Solid State Commun.* **62**, 833 (1987).
- ⁴W. L. Mochan and R. G. Barrera, *Phys. Rev. Lett.* **55**, 1192 (1985).
- ⁵A. Selloni, P. Marsella, and R. Del Sole, *Phys. Rev. B* **33**, 8885 (1986).
- ⁶F. Manghi, E. Molinari, R. Del Sole, and A. Selloni, *Surf. Sci.* **189/190**, 1028 (1987).
- ⁷F. Manghi, E. Molinari, R. Del Sole, and A. Selloni, *Surf. Sci.* **211/212**, 518 (1989).
- ⁸F. Manghi, E. Molinari, R. Del Sole, and A. Selloni, *Phys. Rev. B* **39**, 13005 (1989).
- ⁹F. Manghi, R. Del Sole, A. Selloni, and E. Molinari, *Phys. Rev. B* **41**, 9935 (1990).
- ¹⁰V. L. Berkovits, I. V. Makarenko, T. A. Minashvili, and V. I. Safarov, *Solid State Commun.* **56**, 449 (1985).
- ¹¹V. L. Berkovits, L. F. Ivantsov, I. V. Makarenko, T. A. Minashvili, and V. I. Safarov, *Solid State Commun.* **64**, 767 (1987).
- ¹²C. M. Wijers and K. M. E. Emmett, *Phys. Scr.* **38**, 435 (1988).
- ¹³A. Bagchi, R. G. Barrera, and A. K. Rajagopal, *Phys. Rev. B* **20**, 4824 (1979).
- ¹⁴R. Del Sole, *Solid State Commun.* **37**, 537 (1981).
- ¹⁵R. Del Sole, W. L. Mochan, and R. G. Barrera, *Phys. Rev. B* **43**, 2136 (1991).
- ¹⁶J. A. Stratton, *Electromagnetic Theory* (McGraw-Hill, New York, 1941).
- ¹⁷J. Vlieger, *Physica* **64**, 63 (1973).
- ¹⁸B. M. E. van der Hoff and G. C. Benson, *Can. J. Phys.* **31**, 1087 (1953).
- ¹⁹C. M. J. Wijers (unpublished).
- ²⁰J. Grindlay, *Physica* **107A**, 471 (1981).
- ²¹M. S. Hybertsen and S. G. Louie, *Phys. Rev. B* **34**, 5390 (1986).
- ²²F. Bechstedt and R. Del Sole, *Phys. Rev. B* **38**, 7710 (1988).
- ²³W. Kohn and L. J. Sham, *Phys. Rev.* **140**, A1133 (1965).
- ²⁴D. Straub, M. Skibowski, and F. Himpfel, *J. Vac. Sci. Technol. A* **3**, 1484 (1985); *Phys. Rev. B* **32**, 5237 (1985).
- ²⁵T. Riesterer, P. Perfetti, M. Tschudy, and B. Rehil, *Surf. Sci.* **189/190**, 795 (1987); B. Rehil, T. Riesterer, M. Tschudy, and P. Perfetti, *Phys. Rev. B* **38**, 13456 (1988).
- ²⁶R. Del Sole and E. Fiorino, *Phys. Rev. B* **29**, 4631 (1984).
- ²⁷E. Fiorino and R. Del Sole, *Phys. Status Solidi B* **119**, 315 (1983).
- ²⁸W. Hanke and L. J. Sham, *Phys. Rev. B* **21**, 4656 (1980).
- ²⁹R. Del Sole, *Surf. Sci.* **123**, 231 (1982).
- ³⁰C. M. Wijers and R. Del Sole, *Phys. Scr.* **T25**, 325 (1989).
- ³¹F. Bechstedt, R. Del Sole, and F. Manghi, *J. Condens. Matter* **1**, SB75 (1989); F. Bechstedt and R. Del Sole, *Solid State Commun.* **74**, 41 (1990).
- ³²Z. H. Levine and D. C. Allan, *Phys. Rev. Lett.* **63**, 1719 (1989).
- ³³R. Del Sole and R. Girlanda, in *Proceedings of the 20th International Conference on the Physics of Semiconductors, Thessaloniki 1990*, edited by E. M. Anastassakis and J. D. Joannopoulos (World Scientific, London, 1990), p. 1883.